# Comparison of Energy Deposition Modes in Polyethylene Films by Megaelectronvolt Range Neutrons, Electrons, Protons, and α Particles as Monitored by Covalent Attachment of Doped Pyrene Molecules†

**Gerald O. Brown,§ Noel A. Guardala,‡ Jack L. Price,‡ and Richard G. Weiss*,§**

*Department of Chemistry, Georgetown University, Washington, D.C. 20057-1227, and Carderock Division, Naval Surface Warfare Center, 9500 MacArthur Boulevard, West Bethesda, Maryland 20817*

*Received: October 22, 2002; In Final Form: January 3, 2003*

The selectivity and efficiency of the covalent attachment of pyrene molecules to chains of polyethylene (PE) films by various forms of ionizing radiation (neutrons, electrons, protons, and α particles) have been examined while varying several aspects of the reactions. The results are compared with those from irradiations by >300 nm (<4.1 eV) photons. For each type of ionizing radiation, selectivity and attachment efficiency (*G*) increase with decreasing particle dose. Bombardment by protons, α particles, and electrons produces significant amounts of pyrene molecules attached at two positions, whereas comparable doses of >300 nm (<4.1 eV) photons yield monosubstituted pyrenes only. Higher doses of photons result in attached species that are not pyrenyl in nature. Selectivity is independent of particle kinetic energy in the 3.0−7.0 MeV range for α particles and in the 1.0−4.5 MeV range for protons. Bombardment by ⟨2.0⟩ MeV neutrons is the least efficient of the ionizing radiation sources explored. Selectivity of attachment is independent of PE crystallinity and so is efficiency when protons or α particles are the radiation source. Significant cross-linking and scission of PE chains accompanies the bombardments at higher doses. The nature of the transformation of particle kinetic energy to potential energy and eventually to work as a function of depth of penetration is explored by analyzing individual pyrene-doped PE films that were bombarded in stacks. They indicate that both the selectivity and efficiency of attachment correlate in different ways with the linear transfer of energy to a film. Where direct comparisons are possible, the differing forms of ionizing radiation appear to interact with the polymer matrixes in a somewhat similar manner. However, there are important, subtle differences as well and they are indicated.

## Introduction

Few studies have compared the influence of different forms of ionizing radiation from particle bombardments (i.e., megaelectronvolt-range kinetic energies) and UV/vis photon irradiations (i.e., electronvolt-range potential energies) on the chemical processes that they initiate in organic media. Among these are the γ-radiolyses (i.e., from high-energy photons) and UV/vis photolyses of several types of molecules in liquid organic media performed by Hammond and co-workers in the 1960s.[1] For example, γ-radiolyses and triplet-sensitized irradiations in benzene solutions led to very similar cis−trans steady-state compositions of a series of alkenes, including stilbenes, 1,2-diphenylpropenes, and piperylenes. High *G* values[2] for triplet-state formation during γ-radiolyses were attributed to rapid energy transfer to the alkene that competes with triplet−triplet annihilation reactions within spurs (where the local density of excited-state solvent molecules is high).[3]

We have demonstrated that it is possible to attain selective and efficient attachment of pyrene to polyethylene chains in films using <4.1 eV (>300 nm) photons,[4] as well as megaelectronvolt-range protons.[5] The nature of the major attachment species in the films, a 1-pyrenyl group, is supported by results from UV/vis[6] and ⟨1.3⟩ MeV X-ray irradiations[5c] of pyrene-doped matrixes of solid saturated hydrocarbons. Within the 1.0−4.5 MeV range of protons studied, selectivity of attachment of pyrene to polymer chains was independent of proton kinetic energy but decreased with increasing proton dose.[5] The efficiency of attachment increased somewhat with decreasing polymer crystallinity, and a dependence on crystallinity that could be ascribed to other factors as well was present. Efficiency increased significantly with initial pyrene dopant concentration at high doses and was only slightly dependent on pyrene concentration at low doses. By comparison, attachment selectivity from irradiations with <4.1 eV (>300 nm) *photons* decreased with increasing dose, as well as $O_2$ concentration within the films. Also, because of the biphotonic nature of the attachment process from UV/vis irradiations and the relatively low photon fluxes employed, the efficiency with protons was higher than that with photons.[4b]

Here, we examine the influence of four sources of megaelectronvolt-range ionizing radiation (neutrons, electrons, protons, and α particles) and of varying their kinetic energies and doses on the selectivity and efficiency of pyrenyl attachment to polyethylene chains in films with different crystallinities. We find that particle bombardments produce significant amounts of pyrenyl groups attached at two positions to polymer films in addition to the previously reported monoattachments. The results are compared internally and with those from irradiations by UV/vis (electronvolt-range) photons to determine the degree to which the mechanisms of attachment are dependent on the

† Part of the special issue "George S. Hammond & Michael Kasha Festschrift".

* To whom correspondence should be addressed. Phone: (202) 687-6013. Fax: (202) 687-6209. E-mail: weissr@georgetown.edu.

§ Georgetown University.

‡ Naval Surface Warfare Center.

10.1021/jp022274+ CCC: $25.00 
Published on Web 04/08/2003

**TABLE 1: Properties of PE Films**

| polyethylene | % crystallinity[a] | thickness ($\mu$m)[5b] | density (g cm$^{-3}$)[5b] |
|---|---|---|---|
| PE42 | 42 (24) | 38,76 | 0.918 |
| PE73 | 73 (50) | 20 | 0.945 |
| PE76 | 76 (42) | 13 | 0.952 |

[a] By X-ray diffraction. Values in parentheses by DSC analyses.

source of the deposited energy. In addition, we show that stacks of pyrene-doped polyethylene films provide a histogram of energy deposition by ionizing radiation:[7] individual films within the stacks contain information about particle kinetic energy (via depth of penetration) and dose (via concentrations of attached 1-pyrenyl groups);[5] the particles leave a history of their number and energy within the films.

## Experimental Section

**Materials.** As received PE42 (Sclairfilm 300 LT-1, Dupont of Canada, Mississauga, Ontario), PE73 (type ES-300, Polialden, Petroquimica, Brazil), and PE76 (HDPE 7745,10, Exxon Chemical Co., Baytown Polymers Center-Polyethylene Technology Division, Baytown, TX) films (Table 1) were immersed in several aliquots of chloroform for more than 1 week to remove antioxidants and plasticizers. Pyrene (Aldrich, 99%) was recrystallized from benzene, passed through an alumina column using benzene as eluant, and recrystallized twice from ethanol to yield pale yellow crystals, mp 148.6−149.1 °C (lit.[8] mp 149−150 °C). 1-Ethylpyrene, mp 95−96 °C (lit.[9] mp 94−95 °C), from Molecular Probes and methanol (EM Science, HPLC grade) and chloroform (Fisher, HPLC grade) were used as received.

**Instrumentation for Analyses.** UV/vis absorption spectra were recorded on Perkin-Elmer Lambda-6 and Cary 300 Bio spectrophotometers. Concentrations (±10%) of pyrene within the films before bombardments were determined from the average of the optical densities of three different spots on a film surface and Beer's law using the molar extinction coefficient in petroleum ether at 335 nm, 55 000 M$^{-1}$ cm$^{-1}$.[10] Calculations of concentrations of attached pyrenyl groups in films after bombardments and removal of unattached species (vide infra) were based on 38 970 M$^{-1}$ cm$^{-1}$ for the molar extinction coefficient of 1-ethylpyrene in hexane at 278 nm (determined from a Beer's law plot).

Fluorescence excitation (corrected for detector response) and emission spectra (uncorrected) under vacuum (<$10^{-5}$ Torr) were recorded at a right angle from the back faces of films in a Spex Fluorolog 111 spectrofluorimeter or a Jobin Yvon Spex Fluoromax-2 spectrofluorimeter with 150-W high-pressure xenon lamps and ca. 0.9 nm resolution on both excitation and emission monochromators. Differential scanning calorimetry (DSC) analyses were performed using a TA2910 DSC cell base interfaced to a Thermal Analyst 3100 controller. Samples were placed in crimped aluminum pans, and the apparatus was calibrated with an indium standard. Crystallinity contents in films were determined from powder X-ray diffractograms using a Rigaku R-AXIS image plate system with Cu K$\alpha$ X-rays ($\lambda$ = 1.540 56 Å), and data were processed and analyzed using MDI-Jade (version 5) software. Crystallinities from X-ray analyses (Table 1) differ from the DSC values[11] for reasons that have been discussed elsewhere.[12] The X-ray determined numbers are more reproducible, and they will be used in subsequent analyses.

**Preparation and Bombardment of Pyrene-Doped PE Films.** Pieces of polyethylene film were immersed in chloroform solutions of 0.2 M pyrene for 1 day and dried under a stream of nitrogen, and their surfaces were washed with methanol (a nonswelling solvent) followed by drying under a stream of nitrogen. Following bombardment or irradiation, films were soaked in several aliquots of chloroform until UV/vis absorption and fluorescence spectra of the last chloroform wash showed no pyrene or other unattached aromatic species (usually 2 days). The films were then dried under a stream of nitrogen. Unless indicated otherwise, all reported spectroscopic data on bombarded films were acquired after this extraction process to remove noncovalently attached lumophores.

Uniform beams of 1.0, 2.2, and 4.5 MeV protons and 3.0, 5.0, and 7.0 MeV $\alpha$ particles, produced by a 3MV NEC Pelletron tandem accelerator operated by the Naval Surface Warfare Center (NSWC; Carderock Division, West Bethesda, MD),[13] were passed through a 1 mm aperture in a tantalum foil and swept repeatedly across ca. 1 cm × 1 cm film surfaces. Prior to bombardments, films were placed under ~$10^{-7}$−$10^{-8}$ Torr pressure for at least 5 min; the generator and compartment holding the films were maintained at this pressure during bombardments. Exposure times ranged from 2 to 5 s ($10^9$ $He^{2+}$/cm$^2$ or $H^+$/cm$^2$) to 200−300 s ($10^{13}$ $He^{2+}$/cm$^2$ or $H^+$/cm$^2$); the beam flux was lowered to obtain low doses corresponding to $10^9$ $He^{2+}$/cm$^2$ or $H^+$/cm$^2$.

The dose in gray (1 Gy = 1 J/kg of material) delivered to each film by the protons and $\alpha$ particles was determined from eq 1,[7] where $F$ is the particle fluence in cm$^{-2}$, $E$ is the particle

$$\text{dose (Gy)} = (1.60 \times 10^{-10})FE/(R\rho) \qquad (1)$$

energy in MeV, $R$ is the particle range (i.e., maximum depth of particle penetration) in cm calculated from the TRIM (transport of ions in materials) code,[17] and $\rho$ is the density of the material in g/cm$^3$. Neutron doses were determined by weighting the neutron energies and intensities covering the 0.18−3.7 MeV range and using flux-to-dose conversion factors.[14] In those cases in which the particle is stopped within a film, the dose is based on the volume included within the range.

A uniform 32 MeV beam of electrons was generated using a 7−32 MeV travelling wave linear accelerator (LINAC) operated by the Medical and Industrial Radiation Facility (MIRF) of the National Institute of Standards and Technology, Gaithersburg, MD. Films were flushed with argon for several minutes and sealed in polyethylene bags under argon prior to bombardment. They were bombarded with doses ranging from ~3−1600 kGy corresponding to exposure times of ~1−700 s. The dose deposited per film was determined using the program ESTAR,[15] which calculates the total stopping power for electrons using classical linear energy transfer relationships.[16]

The fast neutron flux in the forward direction subtended by the films was measured experimentally as a function of proton energy by measuring the induced $^7$Be activity in thick $Li_2O$ pellets using the known proton energy losses and ranges.[17] A yield of fast neutrons covering the entire range of incident proton energies capable of producing neutrons from the $^7$Li(p,n) → $^7$Be reaction was then established as a function of proton energy: the maximum incident proton energy available was 5.5 MeV, and 1.89 MeV was the threshold energy for neutron production. The reaction above results in neutrons with 0.18−3.7 MeV energies that are emitted at zero degrees with respect to the incoming protons and intensity maxima at 525 keV and 3.3 MeV. From an average of these energies and the neutron fluence, 2.13 × $10^{13}$ neutrons/cm$^2$, the stack of 10 exposed PE films in the air received a total dose of 141 Gy (or 14 Gy per film) during the 14 h exposure.

Methods for UV/vis irradiation of pyrene-doped PE films have been described elsewhere.[4b]

**Fluorescence Decay Data.** Fluorescence decay histograms were recorded on an Edinburgh Analytical Instruments model FL900 time-correlated single photon counting system using $H_2$ as the lamp gas. Films, in evacuated ($<10^{-5}$ Torr) flattened quartz capillaries, were aligned at $\sim 45°$ to the incident radiation. Emission was detected at a right angle from the back face of the sample. An instrument response function was determined using Ludox as scatterer and without polarizers. Data were collected in 1023 channels (0.504 ns/channel), and $\sim 10^4$ counts were collected in the peak channel (beyond the scatter peak, if present) unless indicated otherwise.

A range from time = 0 (a channel before the onset of the instrument-response signal) to at least 2 decades of decay from the peak channel was included in the analyses. All curve fitting and deconvolution used a nonlinear least-squares routine with software supplied by Edinburgh Instruments. A small "scatter peak" of very short duration was present in the decay profiles of some of the films. Each is omitted from reported fits but has been included in the analyses of the histograms. Goodness of fit was assessed from $\chi^2$ values and plots of residuals. $\chi^2$ values of $<1.2$ were deemed acceptable if no systematic deviation in the residual plot was apparent. Initially, monoexponential fits were attempted. If unacceptable for either reason, two exponential terms and so on were used until satisfactory fits were achieved.

## Results and Discussion

**Criteria for Attachment Efficiency and Selectivity.** Lamotte and co-workers[18] have shown that irradiation of pyrene with ultraviolet photons in solid and liquid alkane solutions yields 1-alkylpyrenes in addition to other photoproducts the number and type of which depend on photon wavelength. The 1-position of ground-state pyrene is known to be the most reactive toward radicals (and cations),[19] and ab initio calculations indicate that it is also the most reactive site of the first excited singlet state.[6] We have also demonstrated that $>300$ nm radiation can lead to attachment of pyrene to chains of PE films[4] and *n*-alkanes.[6] In *n*-alkane matrixes, the mode of attachment is very dependent on solvent phase, pyrene concentration, radiation wavelength, and alkane chain length; pyrene molecules reside and react preferentially at interfaces between lamellae in solid phases of long-chained *n*-alkanes.[6]

The selectivity of attachment of pyrene to chains of PE is based on several dynamic and spectroscopic signatures of bombarded or irradiated (and exhaustively extracted) films. They include the following: (1) the position and shape of UV/vis absorption and excitation/emission spectra (note that the spectra of 1-ethylpyrene and other 1-alkylated pyrenes are bathochromically shifted by $\sim 7$ nm relative to spectra of pyrene[20] and the 0−0 absorption band of dialkylated pyrene is red-shifted from that of pyrene by ca. 11 nm[21]); (2) excited singlet lifetimes of the attached lumophores (e.g., the singlet lifetime of 1-ethylpyrene doped in PE, ca. 190 ns,[22] is significantly shorter than that of pyrene, ca. 300 ns,[22] and significantly longer than that of dialkylated pyrenes, ca. 150 ns). Attachment is considered most selective when the excitation and emission spectra of the attached lumophores have the same shape, position, and temporal decay characteristics as 1-alkylated and disubstituted pyrenes.[22]

Attachment efficiencies are based on *G*-values,[2] in analogy with quantum yields of reactions initiated by electronvolt-range photons.[23] They refer primarily to estimated concentrations of 1-pyrenyl groups covalently attached to polymer chains. It is assumed that absorptions by films at 343 nm are due only to 1-pyrenyl groups although dialkylated pyrenyl groups absorb somewhat at this wavelength as well.

**SCHEME 1: Principal Steps of the Proposed Mechanism for Attachment of Pyrene to Polyethylene Using Ionizing Radiation**[a]

$$\mathrm{PE} \xrightarrow{\textit{Ionizing Radiation}} \mathrm{R}^{\neq} + \mathrm{H}^{\neq} \quad (2)$$

$$\mathrm{PyH} \xrightarrow{\textit{Ionizing Radiation}} {}^1\mathrm{PyH}^* + {}^3\mathrm{PyH}^* + \mathrm{PyH}^{\cdot-} + \mathrm{PyH}^{\cdot+} \quad (3)$$

$$\mathrm{R}^{\neq} + \mathrm{PyH} \longrightarrow \mathrm{R\text{-}PY\text{-}H}^{\neq} \quad (4)$$

$$\mathrm{R\text{-}PY\text{-}H}^{\neq} \longrightarrow \mathrm{PyR} + \mathrm{H}\cdot \quad (5)$$

$$\mathrm{R}^{\neq} + \mathrm{R}^{\neq} \longrightarrow \mathrm{R\text{-}R} \quad (6)$$

$$\mathrm{H}\cdot + \mathrm{H}\cdot \longrightarrow \mathrm{H\text{-}H} \quad (7)$$

[a] When an intermediate on one side only of an equation has $\neq$ (symbolizing + or •), an electron (from pyrene, the polyethylene matrix, or a species derived from them) must be added to balance charges.

**Mechanism of Pyrene Attachment by Ionizing Radiation.** Due to the nearly indiscriminate nature of interactions of megaelectronvolt particles with the host and the guest, the much larger concentrations of C−H and C−C bonds in polyethylene chains make them the much more likely loci for initial energy deposition (Scheme 1). For instance, from the cross sections for interaction of carbon and hydrogen nuclei with neutrons and the weight percentage of pyrene in PE42, only $\sim 0.3\%$ of the energy deposited by ionizing radiation is directly transferred to pyrene molecules.[14] Pyrene attachment follows from the almost simultaneous formation of pyrene excited states and radicals[24] and polymer-based radicals (steps 2 and 3). Polymer radicals can add to ground-state pyrene molecules, followed by formal loss of H• (steps 4 and 5) to yield attached pyrenyl groups. Polymer radicals can also combine to cross-link (step 6) (or disproportionate, leading to scission), and H• radicals can combine to form molecular hydrogen (step 7).[25−27]

**Bombardment of Pyrene-Doped PE Films with 32 MeV Electrons and ⟨2.0⟩ MeV Neutrons and Irradiations with <4.1 eV Photons (Low Linear Energy Transfer (LET) Particles).** Because the penetration depth of 32 MeV electrons, 12.8 cm,[15] is much greater than that of the positively charged particles and neutrons have a $<7\%$ probability[28] of being scattered within our stack of PE films, both of these particles deposit much less energy per unit distance of PE film than do protons and α particles. As such, the former are classified as low linear energy transfer (LET) species, and the latter are considered high LET species; their distributions of energies along their "tracks" are very different and can lead to different primary chemical events.[29] Our results indicate that these deposition modes reduce the local concentration of radicals near tracks as the neutrons (and perhaps electrons) pass through the medium and may change the distribution of energy of the secondary radiation that they create. Figure 1 demonstrates that the selectivity of pyrene attachment decreases with increasing electron dose. The emission spectrum is like that of 1-ethylpyrene at low dose and develops a progressively more pronounced broad underlying emission (including a small excimer-like band at ca. 470 nm) at higher doses. The conclusion from Figure 1 is supported by the marked decrease in both the relative percentage and value of the principle decay component of the fluorescence ($\tau_1$) with increasing dose (Table 2) and the increases in cross-linking and scission of polyethylene chains indicated by differential scanning calorimetry thermograms (see Figure 1 of Supporting Information).

Uncharged neutrons do not ionize matter directly. Instead, they interact almost exclusively with atomic nuclei[30] to produce ionized species such as protons and heavier positive ions that are responsible for the observed chemical effects in materials.

**TABLE 2: Fluorescence Decay Data for $10^{-2}$ mol/kg of Pyrene or 1-Ethylpyrene in PE42 Films Bombarded with Particles or Irradiated with >300 nm (<4.1 eV) Photons at Various Doses**

| dopant | particle | $\lambda_{ex}$ (nm) | $\lambda_{em}$ (nm) | dose (kGy) | $\tau_1$ (ns)[a] | $\tau_2$ (ns)[a] | $\tau_3$ (ns)[a] | $\chi^2$ |
|---|---|---|---|---|---|---|---|---|
| pyrene | 32 MeV electrons | 343 | 377 | 3.18 | 194.5 ± 0.6 (88) | 65.8 ± 1.1 (10) | 4.9 ± 1.3 (2) | 1.143 |
| | | 360 | 381 | 13.0 | 152.0 ± 0.8 (51) | 24.3 ± 1.3 (44) | 1.5 ± 0.9 (3) | 1.099 |
| | | 343 | 377 | 1600 | 150.8 ± 0.2 (71) | 54.6 ± 1.3 (27) | 5.0 ± 1.6 (2) | 1.185 |
| pyrene | 2.2 MeV protons | 343 | 377 | 0.0344 | 189.4 ± 0.5 (90) | 51.4 ± 1.8 (7) | 4.9 ± 1.2 (3) | 1.116 |
| | | 343 | 377 | 344 | 106.4 ± 0.8 (67) | 32.8 ± 1.2 (23) | 2.8 ± 0.6 (10) | 1.088 |
| pyrene | 7.0 MeV α particles | 343 | 377 | 0.231 | 184.3 ± 0.5 (91) | 52.1 ± 1.4 (6) | 3.6 ± 1.7 (3) | 1.159 |
| | | 343 | 377 | 351 | 182.3 ± 1.2 (75) | 71.7 ± 1.7 (21) | 6.6 ± 0.3 (4) | 1.182 |
| | | 360 | 381 | 351 | 145.5 ± 0.5 (73) | 50.8 ± 1.5 (23) | 7.0 ± 0.4 (4) | 1.259 |
| pyrene | <4.1 eV photons | 343 | 377 | ~(2−7) × $10^3$ [5b] | 195.0 ± 0.5 (94) | 26.9 ± 0.9 (4) | 0.4 ± 0.1 (2) | 1.166 |
| | | 360 | 381 | ~(2−7) × $10^3$ [5b] | 191.4 ± 1.1 (81) | 41.8 ± 3.5 (10) | 13.2 ± 0.6 (9) | 0.964 |
| 1-ethylpyrene[b] | | 343 | 377 | 0 | 194.0 ± 0.3 (100) | | | 1.094 |
| 1-ethylpyrene[c] | 2.2 MeV protons | 343 | 377 | 3.44 | 166.3 ± 0.7 (74) | 61.1 ± 0.7 (24) | 0.5 ± 0.1 (2) | 1.314 |
| | | 360 | 381 | 3.44 | 155.9 ± 1.0 (64) | 71.4 ± 0.9 (35) | 5.3 ± 0.3 (1) | 1.398 |

[a] Numbers in parentheses are relative percentages of each component. [b] $10^{-6}$ mol/kg of 1-ethylpyrene in PE42. [c] $10^{-2}$ mol/kg of 1-ethylpyrene in PE42.

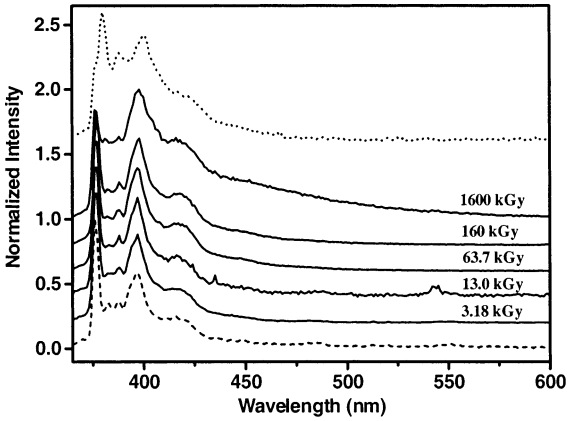


**Figure 1.** Intensity normalized emission spectra ($\lambda_{ex}$ = 343 nm) of (—) $10^{-2}$ mol/kg of pyrene in PE42 films bombarded with 32 MeV electrons as a function of dose and normalized emission spectra ($\lambda_{ex}$ = 360 nm) of (•••) $10^{-2}$ mol/kg of pyrene in PE42 bombarded with 32 MeV electrons (dose = 13.0 kGy) and (- - -) $10^{-6}$ mol/kg of 1-ethylpyrene in PE42.

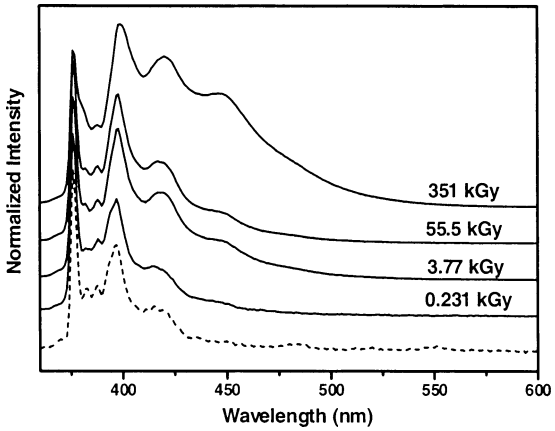


**Figure 2.** Intensity normalized emission spectra ($\lambda_{ex}$ = 343 nm) (—) of $10^{-2}$ mol/kg of pyrene in PE42 bombarded with 7.0 MeV α particles as a function of dose and (- - -) of $10^{-6}$ mol/kg of 1-ethylpyrene in PE42.

As such, the transfer of energy to the PE films by neutrons must be described by a probability function for collisions with carbon and hydrogen nuclei.[14] Because the cross sections for those collisions are very small, very large neutron fluences are required to deposit doses large enough to effect observable changes. The fluence striking our stack of 10 $10^{-2}$ mol/kg of pyrene in PE42 films, 2.13 × $10^{13}$ neutrons/cm$^2$, corresponds to a total dose of 141 Gy (or 14 Gy per film). A barely detectable amount of 1-pyrenyl emission was detected from the total stack (see Figure 2 of Supporting Information). From it, an estimated detection limit of 0.005 OD units in UV/vis absorption spectra, and the lack of detectable absorbance from the strong band of pyrenyl groups near 278 nm (assuming $\epsilon$ = 38 970 M$^{-1}$ cm$^{-1}$), an upper limit of 2 × $10^{-6}$ mol/kg is placed on the concentration of attached 1-pyrenyl groups. The low efficiency of pyrenyl attachment by neutrons is not a consequence of the bombardment having been conducted in air. The presence of air affects selectivity but appears to have little effect on efficiency.[4b]

For very different reasons, the deposition of energy into pyrene-doped PE films from UV/vis (electronvolt-range) photons may be also described by a probability function. Under the conditions of our irradiations, photons are either absorbed completely in one event or transmitted through the material.[31] The most common form of that function is Beer's law in which the molar extinction coefficient is related to the cross section for absorption. On that basis, the dose from >300 nm photons has been estimated for a PE42 film containing $10^{-2}$ mol/kg of pyrene[5b] and is included in Table 4. The corresponding *G* value does not consider the fact that each attachment event requires *two* photons in the wavelength range employed.[18]

**Bombardment of Pyrene-Doped PE Films with Protons and α Particles (High LET Particles).** The similarity of the shapes and positions of the emission spectra from pyrene-doped PE films exposed to comparable doses of 3.0, 5.0, and 7.0 MeV α particles (Figure 3 of Supporting Information) indicates that selectivity of attachment does not depend discernibly on the kinetic energy of the individual particles. However, as shown in Figure 2, attachment selectivity does decrease with increasing dose. The shapes of the emission spectra at $\lambda_{ex}$ = 343 nm change from being like that of 1-ethylpyrene at the lower doses to one with a broad underlying band centered at ca. 470 nm, attributed primarily to an "interchain" excimer,[5] at the highest dose. The longest fluorescence temporal decay constant, $\tau_1$, is very similar in magnitude to that of 1-ethylpyrene and is attributed to singly attached pyrenyl units within the polyethylene matrix. Consistent with the conclusions derived from the steady-state emission spectra in Figure 2, the relative contribution of $\tau_1$ to the total decay decreases markedly from the lowest to the highest dose (Table 2).

In addition, the decrease in $\tau_1$ to ca. 145 ns at the highest dose when $\lambda_{ex}$ is 360 nm suggests the presence of an additional emitting species that appears to be a doubly attached pyrene. The emission and excitation spectra of the pyrene-doped PE films that had been bombarded by electrons, 1−4.5 MeV protons, and 3−7 MeV α particles were dependent on excitation

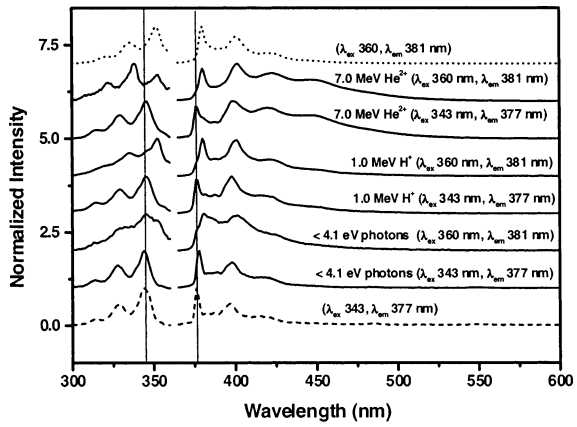


**Figure 3.** Intensity normalized excitation and emission spectra of (—) $10^{-2}$ mol/kg of pyrene in PE42 films after bombardment by 7.0 MeV α particles (dose = 351 kGy), 1.0 MeV protons (dose = 300 kGy), and <4.1 eV photons (dose = $2 \times 10^6$ kGy), (···) $10^{-2}$ mol/kg of 1-ethylpyrene in PE42 bombarded with 2.2 MeV protons (dose = 0.0344 kGy), and (- - -) unirradiated $10^{-6}$ mol/kg of 1-ethylpyrene in PE42 film. The vertical lines are at 343 and 377 nm.

and emission wavelength, respectively. Examples of films bombarded by 1.0 MeV protons and 7.0 MeV α particles are included in Figure 3. For instance, their emission spectra are shifted bathochromically by 4 nm (note the 377 and 381 nm emission bands) when the excitation is changed from 343 to 360 nm. The absorption and emission spectra of pyrene are known to shift incrementally to longer wavelengths as the number of alkyl substituents on the rings increases.[21] In addition, the ~150 ns values for $\tau_1$ from the pyrene-doped and bombarded films in Table 2 are ca. 40 ns shorter than that of a 1-alkylated pyrene,[22] and they are comparable to the $\tau_1$ value of a PE42 film doped with $10^{-2}$ mol/kg of *1-ethylpyrene* and bombarded with 2.2 MeV protons (Table 2). We attribute the red-shifted emissions at $\lambda_{ex}$ 360 nm to *doubly* alkylated pyrenyl groups (that are probably attached to *two* polyethylene chains) when attachment is induced by bombardments with the charged particles. Although emission spectra from pyrene-doped films irradiated with <4.1 eV photons are somewhat like those above when $\lambda_{ex}$ is 360 nm, the principal fluorescence decay constant remains ~190 ns; *there is no evidence for disubstituted pyrenyl species when films are irradiated with high doses of <4.1 eV photons.*[4b] Our calculations[6] indicate that the carbon atom at the 6-position of 1-ethylpyrene is most susceptible to radical (or cationic) attack.

One or two cyclohexane solvent molecules are reported to be attached to each pyrene molecule upon irradiation with 185 nm (6.7 eV) photons, and each attachment requires absorption of only one photon.[18b] When the wavelength was increased to >240 nm (<5.1 eV), only photoproducts with one cyclohexane per pyrene molecule were detected, but each attachment requires absorption of two photons.[18] In addition, upon exposure to broadband ⟨1.3⟩ MeV X-rays, pyrene in solid orthorhombic heneicosane ($C_{21}H_{44}$) yields mono- and disubstituted products, but pyrene in liquid cyclohexane yields products with only one solvent molecule attached.[5c]

The ratios of emission intensities ($I_{377}/I_{381}$) at 377 nm ($\lambda_{ex}$ = 343 nm, attributed to monosubstituted pyrenyl groups) and at 381 nm ($\lambda_{ex}$ = 360 nm, attributed to disubstituted pyrenyl groups) in bombarded pyrene-doped PE42 films are compared in Table 3. The ratio in one film reports the mole fraction of each attached species relative to the other films. The ratios from <4.1 eV photon irradiations of the same films are included for comparison, although they cannot be attributed to the same

**TABLE 3: Ratios of Emission Intensities ($I_{377}/I_{381}$) at 377 nm ($\lambda_{ex}$ = 343 nm) and at 381 nm ($\lambda_{ex}$ = 360 nm) from $10^{-2}$ mol/kg of Pyrene in PE42 Films Bombarded with Charged Particles and Irradiated with <4.1 eV Photons and from $10^{-6}$ mol/kg of 1-Ethylpyrene in PE42 (without Irradiation or Bombardment)**

| particle type | energy (MeV) | range (μm)[a] | film thickness (μm) | dose (kGy) | $I_{377}/I_{381}$ |
|---|---|---|---|---|---|
| proton | 1.0 | 21 | 76 | 30 | 2.3 |
| proton | 2.2 | 81 | 76 | 34 | 1.6 |
| proton | 4.5 | 282 | 38 (film 2)[b] | 22 | 0.96 |
| proton | 4.5 | 282 | 38 (film 4)[b] | 27 | 0.95 |
| proton | 4.5 | 282 | 38 (film 8)[b] | 112 | ca. 0.6[c] |
| α particle | 3.0 | 14 | 38 | 13 | 1.9 |
| α particle | 5.0 | 31 | 38 | 36 | 1.9 |
| α particle | 7.0 | 54 | 38 | 29 | 2.0 |
| electron | 32.0 | $12.8 \times 10^4$ | 38 | 14 | 2.5 |
| photon[d] | $<4.1 \times 10^{-6}$ | | 76 | ~(2−7) × $10^3$ | 5.3 |
| 1-ethylpyrene[e] | | | 76 | | 4.7 |

[a] Proton and α particle ranges were calculated using the TRIM code,[17] and electron ranges were calculated using the ESTAR program.[15] [b] Position of film in a stack of eight films. [c] Includes emissions from secondary reaction products. [d] See text for attributions. [e] $10^{-6}$ mol/kg of 1-ethylpyrene in PE42.

species at 381 nm. The trend in $I_{377}/I_{381}$ at similar low doses suggests that attachment of pyrene at two positions is favored by bombardment with protons of higher kinetic energy. By comparison, $I_{377}/I_{381}$ (~2) does not change with the kinetic energy of α particles, and their ratio is very close to those from films bombarded with 1.0 MeV protons or 32 MeV electrons. The similarity among these ratios is surprising considering the fact that electrons are low LET particles and protons and α particles are high LET particles. As a result, the distributions of energies of secondary electrons[32] (and the "bremsstrahlung" and Compton radiations that eventually follow[30]), created as these particles decelerate within a PE film, should be very different.[29] In all cases, these ratios are much lower than that from the film irradiated with <4.1 eV photons (in which the emitting species at $\lambda_{ex}$ = 381 nm is not a disubstituted pyrene[4b]) or from 1-ethylpyrene doped in PE42.

Greater selectivity of attachment is expected at lower doses of a charged particle, regardless of its type and kinetic energy. At higher doses, the probability of track overlap increases and, with it, the probability for secondary reactions.[29] For instance, the probability of overlap of radiation fields from randomly deposited 1.0 MeV proton tracks with 1.5 nm radii at the point of entry into a film[33] is calculated[34] to be almost zero at $\leq 10^{12}$ $H^+/cm^2$ and 16% at $10^{13}$ $H^+/cm^2$ fluences.[5b] Thus, higher doses lead to the *sequential* generation of radicals and ions in a unit volume within a film.

**Efficiency of Pyrene Attachment in PE Films of Different Crystallinity Using Various Forms of Ionizing Radiation.** Despite the scatter in the data, a plot of *G* for monoattachment of pyrenyl groups versus dose from bombardment by neutrons, electrons, protons, and α particles (Figure 4b) demonstrates that the efficiency of attachment decreases as the dose increases. However, Figure 4a suggests that, in part, the decreases in *G* at higher doses are a consequence of decreased availability of free pyrene molecules. The larger the fraction of pyrene attached is, the less likely it is that incoming particles will be able to effect additional monoattachments. At the same time, the probabilities of secondary events involving attached pyrenyl groups (as noted above) and combinations and disproportionations of pairs of radical chains will increase. This trend is most evident for the stack of eight films bombarded with 4.5 MeV protons. The small increases in dose between the second and

**TABLE 4: Comparison of 1-Pyrenyl Attachment Efficiencies (*G*) upon Bombardment of $10^{-2}$ mol/kg of Pyrene in PE42 Films by High-Energy Particles and >300 nm (<4.1 eV) Photons**

| particle type | total film thickness ($\mu$m) | kinetic energy (MeV) | penetration range (cm) | dose (kGy)[a] | $G$ ($\mu$mol/J) | % attached within the stopping distance |
|---|---|---|---|---|---|---|
| electrons | 38 | 32 | 12.8 | 3.18 | 0.035 | 1.1[d] |
| protons | 76 | 1.0 | $21 \times 10^{-4}$ | 300 | 0.01 | 66 |
| | 76 | 2.2 | $81 \times 10^{-4}$ | 10.9 | 0.10 | 11 |
| | 114 | 2.2 | $81 \times 10^{-4}$ | 7.1 | 0.05 | 4 |
| | 343 | 4.5 | $282 \times 10^{-4}$ | 3.4 | 0.04 | 1.8 |
| | 38 (film 1 of 8) | 4.5 | $282 \times 10^{-4}$ | 19.5 | 0.05 | 7 |
| | 38 (film 2 of 8) | 4.5 | $282 \times 10^{-4}$ | 22.3 | 0.06 | 11 |
| | 304 (8 films) | 4.5 | $282 \times 10^{-4}$ | 300 | 0.03 | 90 |
| $\alpha$ particles | 38 | 3.0 | $14 \times 10^{-4}$ | 13.0 | 0.03 | 9.5 |
| | 76 | 5.0 | $31 \times 10^{-4}$ | 70.4 | 0.01 | 21 |
| | 38 (film 1 of 2) | 7.0 | $54 \times 10^{-4}$ | 115 | 0.024 | 28 |
| | 38 (film 2 of 2) | 7.0 | $54 \times 10^{-4}$ | 151 | 0.022 | 24 |
| neutrons | 76 | $\langle 2.0 \rangle$ | *b* | 0.141 | <0.013[c] | 0.02[d] |
| <4.1 eV photons[5b] | 76 | $\langle 4.0 \times 10^{-6} \rangle$ | *b* | $\sim(2-7) \times 10^3$ | $\sim(5-30) \times 10^{-5}$ | 6.1[d] |

[a] Calculations based on the part of the film within the penetration range when particles stopped within a film. [b] Based on probability rather than range; see text for details. [c] Assuming an upper limit of $2 \times 10^{-6}$ mol/kg for attached 1-pyrenyl groups. [d] Particles/photons not stopped within film thickness.

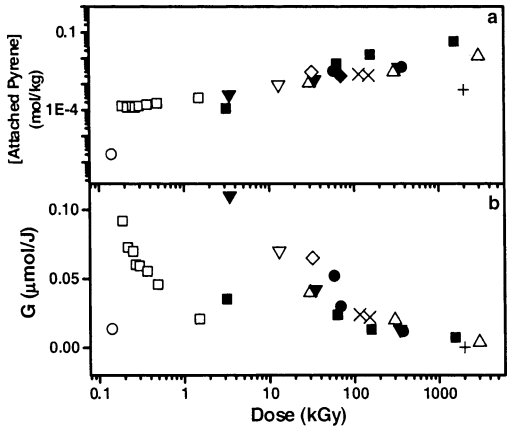


**Figure 4.** Semilog plots of (a) estimated concentrations of attached pyrenyl groups and (b) *G* values versus dose for individual or stacks of bombarded or irradiated $10^{-2}$ mol/kg of pyrene-doped PE42 films: (■) 32 MeV electrons; (△) 1.0 MeV protons; (▼) 2.2 MeV protons; (◇) 4.5 MeV protons, individual films; (□) 4.5 MeV protons, individual (38 $\mu$m) films in a stack of eight; (▽) 3.0 MeV $\alpha$ particles; (◆) 5.0 MeV $\alpha$ particles; (●) 7.0 MeV $\alpha$ particles, individual films (×) 7.0 MeV $\alpha$ particles, individual (38 $\mu$m) films in a stack of two; (○) $\langle 2 \rangle$ MeV neutrons; (+) <4.1 eV photons.

sixth films of the stack and the large decreases in *G* indicate that availability of pyrene molecules is not the only factor at play here (see Figure 4 of Supporting Information). We conjecture that the distribution of energies of secondary electrons in spurs also changes with penetration depth and that the energy distribution at smaller penetration depths promotes attachment more efficiently than that at larger ones; such a dependence of distribution of radiation on depth of particle penetration is also consistent with the trend of $I_{377}/I_{381}$ ratios reported in Table 3.[32]

The *G* values from electron bombardments are comparable to those from proton and $\alpha$ particle bombardments and somewhat larger than those from neutron bombardments (Table 4). This result was not expected because positively charged ions are more efficient cross-linking agents than electrons[35] and the distribution of initial chemical events in PE chains (note C—H and C—C bond cleavages) caused by low and high LET particles are different.[29] All of our PE films appeared to be cross-linked to some extent after bombardment. Those that were bombarded with high doses contained large amounts of polymer that could not be dissolved in hot xylene although the same films were completely soluble prior to bombardment. In addition, melting transitions in DSC thermograms of films bombarded at high doses were slightly narrower and their melting temperatures were somewhat lower than those of unbombarded samples (See, for example, Figure 1 of Supporting Information).

The efficiency of attachment upon irradiation of pyrene-doped PE films with UV/vis (<4.1 eV, >300 nm) photons[5b] is lower than those of the charged particles (Table 4). However, these comparisons are very difficult to quantify because the mechanism of attachment by >300 nm radiation involves *sequential* absorption by two photons and, therefore, its efficiency depends acutely on the flux. In addition, all of the photon energy is deposited initially into the pyrene molecules within a film, while the vast majority of the energy from the particles is deposited initially into the polyethylene matrix. Regardless, differences between the photon- and particle-induced attachments at one dose are evident in the lower degree of cross-linking in films exposed to photons. In addition, at photon doses at which selectivity of attachment is high (Table 2), comparable electron doses lead to very poor selectivity.

These results are consistent with the deposition of energy from UV photons directly into pyrene molecules and the dissipation of that excitation energy predominantly by radiative and nonradiative (heating) processes that regenerate the ground states of pyrene. Under our conditions of low photon flux, only a very small fraction of the electronically excited pyrene molecules absorb a second photon and are capable of reacting with PE chains.[6,18] By contrast, bombarding particles, especially charged ones, interact almost indiscriminately with PE chains and pyrene molecules according to their relative populations so that attachment (as well as cross-linking and scission of chains)[29,36] is possible without electronic excitation of pyrene molecules (steps 2, 4, and 5 of Scheme 1).

The dependence of pyrene attachment efficiency on the type of ionizing radiation and PE crystallinity are summarized in Table 5. The similarity of emission spectra of $10^{-2}$ mol/kg of pyrene in PE42 and PE73 films bombarded with *comparable doses* of electrons and $\alpha$ particles (Figures 5 and 6 of Supporting Information) indicates that PE crystallinity does not have a significant influence on attachment selectivity. Except for electrons, the efficiency of attachment does not appear to depend on crystallinity either. This result was unexpected because it is known that pyrene molecules cannot reside in the crystalline regions of polyethylene.[37] Therefore, the greater the degree of

**TABLE 5: 1-Pyrenyl Attachment Efficiencies (*G*) upon Bombardment of $10^{-2}$ mol/kg of Pyrene in PE Films of 42%, 73%, and 76% Crystallinity by High-Energy Particles**

| polyethylene | total film thickness ($\mu$m) | particle type | kinetic energy (MeV) | dose (kGy)[a] | *G* ($\mu$mol/J) |
|---|---|---|---|---|---|
| PE42 | 38 | electrons | 32 | 3.18 | 0.035 |
| PE73 | 20 | electrons | 32 | 3.18 | 0.017 |
| PE42 | 114 | protons | 2.2 | 7.1 | 0.05 |
| PE73 | 80 | protons | 2.2 | 4.6 | 0.04 |
| PE42 | 38 | α particles | 3.0 | 13.0 | 0.03 |
| PE76 | 26 | α particles | 3.0 | 10.6 | 0.04 |

[a] Based on the part of the film within the penetration range when particles stopped within a film. Under our experimental conditions, only the protons and α particles were stopped within the films.

crystallinity in a PE film is, the smaller statistically will be the fraction of radiation that is near pyrene molecules. In addition, our previous work suggested that the efficiency of attachment might be dependent on PE crystallinity.[5] However, these experiments were not conducted at *similar doses* and, therefore, the comparisons were suspect. The current results indicate that the degree to which pyrene molecules are sequestered within one part of the total film volume (within the limited range investigated) does not have a large effect on their ability to suffer attachment.

**Energy Deposition by Charged Particles in Stacks of Pyrene-Doped PE Films.** Many dosimeters for ionizing radiation are based on degrees of color change.[38] They provide information about the total energy deposited, but most cannot distinguish the kinetic energies of the impinging particles. Stacks of PE films are able to do so.

Energy deposition by ionizing radiation can be followed as a function of penetration depth in stacks of pyrene-doped PE films according to dose using the concentrations of attached 1-pyrenyl groups (note optical density changes and the shapes of the emission spectra from the attached species) and energy (using the profiles of attachment concentrations). Also, the latter may be compared with predicted energy deposition profiles calculated by the TRIM code[17] to determine the extent to which the distribution of secondary radiation changes as a particle passes through doped polyethylene.

Plots in Figure 5 demonstrate that the degree of attachment does follow the energy deposition profiles from the TRIM code, although there is a consistent distance offset between the two. A part (but not all) of the discrepancy can be attributed to the depth resolution of the measurements, which is limited by film thickness. In addition, near the depth limit of penetration, where particle velocity is slowing rapidly (i.e., approaching the Bragg maximum[39]), a very large fraction of the kinetic energy is transferred to the matrix. As a result, multiple "spurs"[29] can go deeper into a film than the depth of maximum penetration predicted by the TRIM code for an ion, allowing chemical events to occur in regions beyond which the ion has passed. Many of the displaced electrons (as well as some photons) within the spurs have more than sufficient energy to induce 1-pyrenyl attachment.

The shapes of the emission spectra from these films are also a monitor of energy deposition by the charged particles. For example, the emission spectra from selected individual pyrene-doped PE42 films in a stack of 10 that was bombarded with 4.5 MeV protons at a total dose of 370 kGy are presented (by their order in the stack) in Figure 6. A progressive decrease in attachment selectivity (note loss of the characteristic 377 nm band) is observed as the depth of the protons increases. The emission spectrum of film 7 (located at the end of the penetration

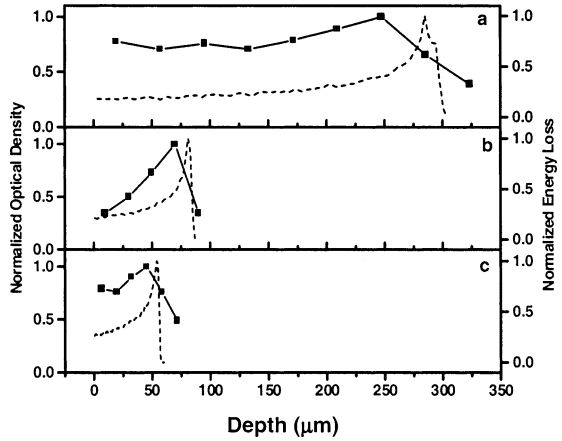


**Figure 5.** Normalized optical density (■, lines represent connectivity between adjacent films only) as a function of depth within stacks of PE films containing $10^{-2}$ mol/kg of pyrene: (a) PE42 bombarded with 4.5 MeV protons (dose = 3.7 kGy); (b) PE73 bombarded with 2.2 MeV protons (dose = 4.57 kGy); (c) PE76 bombarded with 7.0 MeV α particles (dose = 311 kGy). The normalized energy loss profiles for each film (- - -) are shown as well.

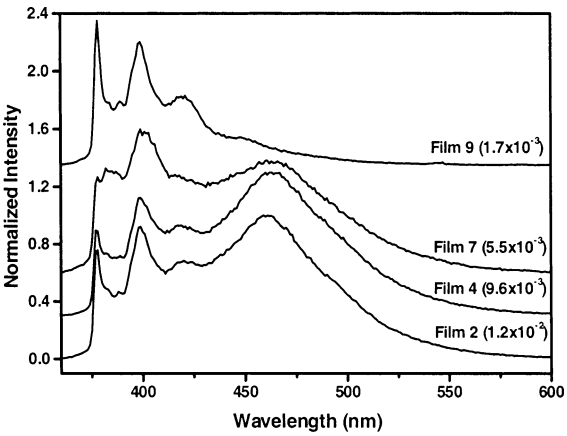


**Figure 6.** Intensity normalized emission spectra of individual films from a stack of $10^{-2}$ mol/kg of pyrene in PE42 films bombarded with 4.5 MeV protons. The numbers increase from films closer to farther from the ion beam, and the concentrations are estimations of attached pyrenyl groups from UV/vis absorption spectra. The numbers in parentheses represent estimated attached pyrenyl group concentrations within each PE42 film.

range predicted for 4.5 MeV protons, where secondary chemical events are more probable[40]) lacks some of the vibronic structure and the sharp band at 377 nm that are characteristic of 1-alkylated pyrene moieties. However, a significant amount of radiation of sufficient energy to effect pyrenyl attachments penetrates the polyethylene beyond the Bragg region, and the emission from film 9 is again like that of a 1-pyrenyl moiety. The radiation does not proceed as far as film 10 upon the basis of its lack of 1-pyrenyl fluorescence.

## Conclusions

We have shown that energy deposition from megaelectronvolt-range neutrons, electrons, protons, and α particles can effect attachment of pyrene molecules to chains of polyethylene films. For each type of particle, selectivity and attachment efficiency (*G*) increase with decreasing particle dose. Bombardment by electrons (and especially) protons, and α particles produces significant amounts of pyrene molecules attached at two positions, whereas >300 nm (<4.1 eV) photons give only monosubstituted pyrenes at low doses and non-pyrenyl second-

ary attachment products at higher doses. This is a clear indication that the modes of attachment initiated by megaelectronvolt-range particles and electronvolt-range photons follow different mechanisms. A key component of this difference is that all of the energy deposited into pyrene-doped PE films by electronvolt-range photons resides initially in the aromatic molecules; the vast majority of the energy deposited by the megaelectronvolt-range particles is located initially in the polymer matrix.

The ratio of mono- to disubstituted attached pyrenyl groups is independent of the kinetic energy of α particles in the 3−7 MeV range examined and is comparable to values found from films bombarded with 1.0 MeV protons or 32 MeV electrons. On this basis, we suggest that similar distributions of secondary radiation are generated as these particles decelerate within the PE films. Of the particles investigated, the least efficient for pyrene attachment were ⟨2.0⟩ MeV neutrons. Attachment selectivity and efficiency are independent of PE crystallinity when protons or α particles are the radiation source, and a small dependence is indicated for 32 MeV electrons.

Regardless of the particle employed, a significant amount of cross-linking and scission of PE chains occurred at high doses. Very little cross-linking and chain scission were found in PE films irradiated at comparable doses with electronvolt-range photons. The distribution of quanta of energy transferred from photon-generated excited states to the polymer matrix because the former decay is very different from the distribution of quanta deposited by megaelectronvolt-range particles directly into the polymer matrix or transferred from it to pyrene molecules.

Because those differences are manifested in depth profiles for reactions within pyrene-doped PE films, stacks of films can provide much greater information about the dose, energy, and type of radiation than many existing dosimeters. The combination of absolute concentration of attached species, "depth profile" for attachment, amount of excimer-like emission, and fraction of disubstituted pyrenyl groups can be used to identify the nature of the ionizing particle, its fluence, and its kinetic energy. Despite this, stacks of pyrene-doped polyethylene films would not be the preferred dosimeter unless very detailed information about the ionizing radiation is desired: the films cannot be analyzed rapidly and calibration curves must be established for their response to different forms of ionizing radiation.

The methodologies employed here should be directly applicable to a wide range of other polymer films. Overall, the results demonstrate that there are subtle differences among the ways that various types of megaelectronvolt-range particles (and electronvolt-range photons) transform their energy to initiate the attachment reactions within polymer films. Those differences constitute a blueprint for future investigations and suggest potential applications. In addition, although the chemistries initiated by photons and ionizing radiation may be the same in some cases, like some of those investigated by Hammond and co-workers four decades ago,[1a,c,3] they clearly are not in others![1b]

**Acknowledgment.** We thank Mr. Mario Lutterotti of Dupont of Canada, Mississauga, Ontario, Prof. Teresa Atvars of the State University of Campinas, Brazil, and Ms. Nancy Richter of the Exxon Chemical Company, Baytown, TX, for supplying the films employed in this work. We also thank Dr. Fred B. Bateman and Mr. Melvin R. McClelland from the Medical and Industrial Radiation Facility (MIRF) of the National Institute of Standards and Technology, Gaithersburg, MD, for performing the electron bombardment experiments. The authors are also grateful to a reviewer for many helpful suggestions. R.G.W. is grateful to the National Science Foundation for financial support.

**Supporting Information Available:** One figure comparing DSC thermograms for an unirradiated PE42 film and 32 MeV electron bombarded (dose = 1600 kGy) PE42; four figures of emission spectra from a stack of 10 $10^{-2}$ mol/kg of pyrene in PE42 films bombarded with ⟨2.0⟩ MeV neutrons and $10^{-6}$ mol/kg of 1-ethylpyrene in PE42, from $10^{-2}$ mol/kg of pyrene in PE76 films after bombardment with 3.0, 5.0, and 7.0 MeV α particles and $10^{-6}$ mol/kg of 1-ethylpyrene in PE76, from $10^{-2}$ mol/kg of pyrene in PE42 and in PE73 films after bombardment by various doses of 32 MeV electrons, and from $10^{-2}$ mol/kg of pyrene in PE42 and in PE73 films after bombardment by various doses of 7.0 MeV α particles; and a figure comparing the percent attached pyrene and *G* values as a function of dose for a stack of eight $10^{-2}$ mol/kg of pyrene in PE42 films bombarded with 4.5 MeV protons at 3.4 kGy (total dose). This material is available free of charge via the Internet at http://pubs.acs.org.

## References and Notes

(1) (a) Caldwell, R. A.; Whitten, D. G.; Hammond, G. S. *J. Am. Chem. Soc.* **1966**, *88*, 2659. (b) Penner, T. L.; Whitten, D. G.; Hammond, G. S. *J. Am. Chem. Soc.* **1970**, *92*, 2861. (c) Penner, T. L.; Hammond, G. S. In *Organic Scintillation and Liquid Scintillation Counting, Proceedings*; Horrocks, D. L., Peng, C. T., Eds.; Academic Press: New York, 1971; p 327.

(2) The dose efficiency, *G*, is defined according to the SI convention as the number of micromoles of species formed per joule of energy deposited. A more commonly used dose efficiency, *G*′, is defined as the number of molecules or events per 100 eV deposited: $G \cong 10G'$.

(3) Hammond, G. S.; Caldwell, R. A.; King, J. M.; Kristinsson, H.; Whitten, D. G. *Photochem. Photobiol.* **1968**, *7*, 695.

(4) (a) Naciri, J.; Weiss, R. G. *Macromolecules* **1992**, *25*, 1568. (b) Brown, G. O.; Zimerman, O. E.; Weiss, R. G. *Polymer* **2002**, *43*, 6495.

(5) (a) Brown, G. O.; Guardala, N. A.; Price, J. L.; Weiss, R. G. *Polym. Prepr.* **2000**, *41*, 1536. (b) Brown, G. O.; Guardala, N. A.; Price, J. L.; Weiss, R. G. *J. Phys. Chem. B* **2002**, *106*, 3375. (c) Brown, G. O.; Guardala, N. A.; Price, J. L.; Weiss, R. G. *An. Acad. Bras. Cienc.* **2003**, *75*, 33.

(6) Zimerman, O. E.; Weiss, R. G. *J. Phys. Chem. A* **1999**, *103*, 9794.

(7) Phillips, G. W.; Readshaw, A. K.; Brown, G. O.; Weiss, R. G.; Guardala, N. A.; Price, J. L.; Mueller, S. C.; Moscovitch, M. *Appl. Radiat. Isot.* **1999**, *50*, 875.

(8) Perrin, D. D.; Amarego, W. L. F. *Purification of Laboratory Chemicals*, 3rd ed.; Pergamon Press: New York, 1988; p 267.

(9) Josephy, E., Radt, F., Eds. *Elsevier's Encyclopedia of Organic Chemistry*; Elsevier: New York, 1940; Series III, Vol. 14, p 379.

(10) *DMS UV Atlas of Organic Compounds*; Plenum Press: New York, 1966; Vol. III, E6/T1.

(11) Zimerman, O. E.; Cui, C.; Wang, X.; Atvars, T. D. Z.; Weiss, R. G. *Polymer* **1998**, *39*, 117.

(12) Luo, C.; Guardala, N. A.; Price, J. L.; Chodak, I.; Zimerman, O.; Weiss, R. G. *Macromolecules* **2002**, *35*, 4690.

(13) Price, J. L.; Land, D. J.; Stern, S. H.; Guardala, N. A.; Cady, P. K.; Simons, D. G.; Brown, M. D.; Brennan, J. G.; Stumborg, M. F. *Nucl. Instrum. Methods Phys. Res.* **1991**, *B56*−*57*, 1014.

(14) Buckner, M. A.; Sims, C. S. *Health Phys.* **1992**, *63*, 352.

(15) Berger, M. J.; Coursey, J. S.; Zucker, M. A. *ESTAR, PSTAR, and ASTAR: Computer Programs for Calculating Stopping-Power and Range Tables for Electrons, Protons and Helium Ions*, version 1.21; National Institute of Standards and Technology: Gaithersburg, MD, 1999; [Online] available at http://physics.nist.gov/Star.

(16) Chatterjee, A. In *Radiation Chemistry: Principles and Applications*; Farhataziz, Rogers, M. A. J., Eds.; VCH Publishers: New York, 1987; p 17.

(17) Ziegler, J. F.; Manoyan, J. M. *Nucl. Instrum. Methods Phys. Res.* **1988**, *B35*, 215.

(18) (a) Lamotte, M.; Joussot-Dubien, J.; Lapouyade, R.; Pereyre, J. In *Photophysics and Photochemistry above 6 eV*; Lahmani, F., Ed.; Elsevier: Amsterdam, 1985; p 577. (b) Lamotte, M.; Pereyre, J.; Lapouyade, R.; Joussot-Dubien, J. *J. Photochem. Photobiol., A* **1991**, *58*, 225.

(19) (a) Mitchell, R. H.; Lai, Y. H.; Williams, R. J. *J. Org. Chem.* **1979**, *44*, 4733. (b) Lapouyade, R.; Pereyre, J.; Garrigues, P. C. *Acad. Sci., Paris, Ser. II* **1986**, *10*, 903.

(20) Berlman, I. B. *Handbook of Fluorescence Spectra of Aromatic Molecules*, 2nd ed.; Academic: New York, 1971; pp 383−384.

(21) De Clercq, M.; Martin, R. H. *Bull. Soc. Chim. Belg.* **1955**, *64*, 367.

(22) Zimerman, O. E.; Weiss, R. G. *J. Phys. Chem. A* **1998**, *102*, 5364.

(23) Verhoeven, J. W. *Pure Appl. Chem.* **1996**, *68*, 2223.

(24) (a) Szadkowska-Nicze, M.; Kroh, J.; Mayer, J. *J. Photochem. Photobiol., A* **1995**, *91*, 241. (b) Szadkowska-Nicze, M.; Kroh, J.; Mayer, J. *Radiat. Phys. Chem.* **1992**, *39*, 23. (c) Szadkowska-Nicze, M.; Mayer, J. *Res. Chem. Intermed.* **2001**, *27*, 823. (d) Johnson, G. R. A.; Willson, A. *Radiat. Phys. Chem.* **1977**, *10*, 89.

(25) Biscoglio, M.; Thomas, J. K. *J. Phys. Chem. B* **2000**, *104*, 475.

(26) Calcagno, L.; Foti, G.; Liccadrillo, A.; Puglosi, O. *Appl. Phys. Lett.* **1987**, *51*, 907.

(27) Chang, Z.; Laverne, J. A. *J. Polym. Sci., Part A: Polym. Chem.* **2000**, *38*, 1656.

(28) The macroscopic cross section ($\Sigma$) is defined as the probability for a neutron being scattered or absorbed within 1 cm of a material. $\Sigma = \rho\sigma$, where $\sigma$ is the microscopic cross section for interaction of a neutron with a nucleus and $\rho$ is the number density of the nucleus in the material. Assuming $CH_2$ for the stoichiometry of PE42 (density = 0.918 g $cm^{-3}$) and taking $\sigma_H = 20$ b and $\sigma_C = 4.7$ b (Grigoriev, I. S., Meilikhov, E. Z., Eds. *Handbook of Physical Quantities*; CRC Press: Boca Raton, FL, 1997; pp1356−1359), an upper limit for $\Sigma$ within a stack of 10 films has been calculated.

(29) (a) Zagorski, Z. P. *Radiat. Phys. Chem.* **2002**, *63*, 9. (b) LaVerne, J. A.; Schuler, R. H.; Foldiak, G. *J. Phys. Chem.* **1992**, *96*, 2588.

(30) Spinks, J. W. T.; Woods, R. J. *An Introduction to Radiation Chemistry*; Wiley: New York, 1964; p 36.

(31) Calvert, J. G.; Pitts, J. N., Jr. *Photochemistry*; Wiley: New York, 1966; p 20.

(32) Drexler, C. G.; DuBois, R. D. *Phys. Rev. A* **1996**, *53*, 1630.

(33) Moscovitch, M.; Emfietzoglou, D. *J. Appl. Phys.* **1997**, *81*, 58.

(34) Horowitz, Y. S.; Moscovitch, M.; Dubi, A. *Phys. Med. Biol.* **1982**, *27*, 1325.

(35) (a) Ikada, Y.; Nakamura, K.; Ogata, S.; Makino, K.; Tajima, K.; Endoh, N.; Hayashi, T.; Fujita, S.; Fujisawa, A.; Masuda, S.; Oonishi, H. *J. Polym. Sci., Part A: Polym. Chem.* **1999**, *37*, 159. (b) Wu, G.; Katsumara, Y.; Kudoh, H.; Morita, Y.; Seguchi, T. *J. Polym. Sci., Part A: Polym. Chem.* **1999**, *37*, 1541. (c) Barkhudaryan, V. G. *Polymer* **2000**, *41*, 2511.

(36) Chapiro, A. *Radiation Chemistry of Polymeric Systems*; Wiley: New York, 1962; p 385 ff.

(37) Phillips, P. J. *Chem. Rev.* **1990**, *90*, 425.

(38) (a) Ohnishi, T.; Hiraoka, E.; Furuta, J. *Radioisotopes* **1978**, *27*, 422. (b) Irie, S.; Yamaguchi, T.; Nakazumi, H.; Kobatake, S.; Irie, M. *Bull Chem. Soc. Jpn.* **1999**, *72*, 1139. (c) Niroomand-Rad, A.; Blackwell, C. R.; Coursey, B. M.; Gall, K. P.; Galvin, J. M.; McLaughlin, W. L.; Meigooni, A. S.; Nath, R.; Rodgers, J. E.; Soares, C. G. *Med. Phys.* **1998**, *25*, 2093.

(39) Olsen, K. J.; Hansen, J. W. *Nucl. Instrum. Methods Phys. Res.* **1984**, *B5*, 497.

(40) Horowitz, Y. S.; Moscovitch, M.; Dubi, A. *Phys. Med. Biol.* **1982**, *27*, 1325.